A FREQUENCY SELECTIVE ABSORBING GROUND PLANE FOR LOW-RCS MICROSTRIP ANTENNA ARRAYS

F. Costa[1, 2, *], S. Genovesi[1, 2], and A. Monorchio[1, 2]

[1]Dipartimento di Ingegneria dell' Informazione, Università di Pisa, Via G. Caruso 16, Pisa 56122, Italy

[2]RaSS National Laboratory, CNIT — Galleria G. B. Gerace 18, Pisa 56124, Italy

Abstract—An efficient strategy for reducing the signature of an antenna is to substitute the conventional solid ground plane with a patterned ground plane thus letting the incoming energy to pass through the structure except over the operating band of the antenna. However, in a real environment, the energy flowing through the *FSS* (Frequency Selective Surface) can be intercepted by eventual scatterers located behind the antenna, so to nullify the RCS (Radar Cross Section) reduction. To overcome this drawback, a novel composite structure is proposed which is able to dissipate such energy by placing a thin absorbing layer below the *FSS* ground. It is shown that a careful analysis has to be performed to accomplish this goal since the transparent antenna array and the backing absorber strongly interact and thus they cannot be separately designed. The optimal value of the foam spacer thickness between the *FSS* ground and the absorbing layer is investigated by an efficient equivalent transmission line approach. Criteria for enlarging the low-RCS band with respect to the free space design are also provided. An antenna array prototype backed by the thin multilayer structure is finally manufactured and tested.

1. INTRODUCTION

The reduction of the structural term of the antenna Radar Cross Section (RCS) involves the shaping of the target surfaces [1, 2] and the use of Radar Absorbing Materials (RAMs) [3–11]. Indeed, it is well known that the antenna RCS significantly contributes to the overall RCS signature of target objects such as naval ships and airborne vehicles. The remaining part of the array RCS is determined by an antenna component which is related to the mismatch at the impedance port [12–14]. A way to reduce the structural component of antenna RCS is to replace the solid ground plane with a band-stop spatial filter allowing the incoming energy to flow through the structure, out of the operating frequency band [15]. This approach is usually applied to reflectarray antennas [15–17] but in our previous works [18, 19] we have shown the possibility of applying the same concept to microstrip antenna arrays. In [19], the metallic ground plane of a printed microstrip array has been replaced by a hybrid metallic *FSS* structure with very low radiation losses. The use of a frequency selective surface as backing plane of an antenna allows the impinging waves to pass through the antenna in the frequency range where the transmission profile of the *FSS* is close to the unity. However, if some scatterers are present behind the low-RCS antenna, the energy is reflected back and the advantages of using the selective ground plane are mostly reduced. A solution to this problem would be the arrangement of some absorbing cones or magnetically loaded materials on the scattering objects. Anyway, these procedures might reveal impracticable for the encumbrance of the absorbing cones and the difficulty of gluing them on curved surfaces as well as for the increase of weight due to the use of magnetic absorbers.

A more compact structure, which is proposed for the first time in this paper, is obtained by placing a low-profile radar absorber employing a resistive *FSS* in the vicinity of the hybrid *FSS* backing plane. Since the metallic *FSS* affects the behavior of the absorbing structure as well as the presence of the radar absorber modifies the impedance seen by the impinging waves, they cannot be designed separately. It is therefore necessary to study the overall composite structure in order to evaluate the optimal FSS configurations and the separation between the antenna and the radar absorber. The paper is organized as follows. In Section 2 the optimal design of the thin absorbing ground plane is addressed by an equivalent circuit model. The absorption properties of the optimized multilayer are provided in Section 3. Finally, the performance of a microstrip antenna on top of the frequency selective absorbing ground plane are evaluated

with respect to the conventional antenna both by simulations and measurements in Sections 4 and 5, respectively.

2. FREE SPACE DESIGN

A reference array has been initially designed for verifying the proposed RCS-reduction technique. It comprises four patch antennas and it is printed on a grounded FR4 dielectric substrate with a thickness equal to 2 mm. The central working frequency is 2.5 GHz and the bandwidth spans from 2.48 GHz to 2.53 GHz. In order to achieve RCS reduction, a periodic pattern is printed on the lower part of the FR4 substrate whereas the patches of the antenna array are printed on the top of it. The unitary reflection band of the FSS matches the antenna resonance frequency in order to allow the proper radiation of the device. Outside the stop-band, the same FSS has to be transparent in order to reduce the overall structural RCS of the array. The FSS comprises an array of slot ring element with the following parameters: $T = 8.0$ mm, $m = 1.0$ mm and $b = 2.0$ mm. A sketch of the employed unit cell with the description of the parameters is shown in the inset of Fig. 2. The optimized hybrid FSS ground presented in [19] and the top layer of the microstrip array are shown in Fig. 1.

In Fig. 2, the reduction of the reflectivity of the modified antenna backed by free space with respect to the reference one with the metallic ground is reported for both polarizations. Some spikes are observed at 2.5 GHz for TE polarization since the electric field is aligned with the patch antenna arrays at the operating frequency.

The result is then compared against the reflection coefficient of the infinite FSS. From the comparison it is possible to notice that
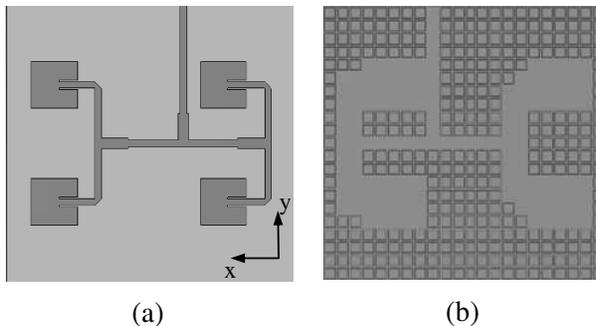

(a)   (b)

Figure 1. (a) Top view and (b) bottom view of the reduced RCS patch array antenna.
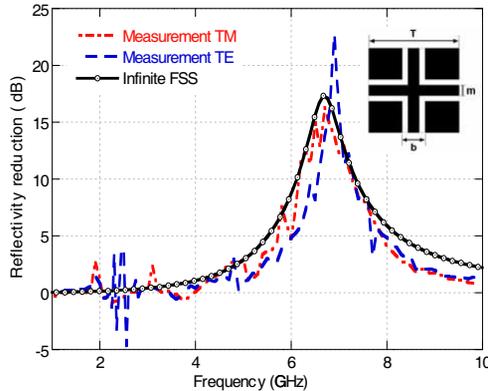
Figure 2. Comparison between the reflection coefficient of the infinite *FSS* and the reduction of the array reflectivity for *TE* (*E* incident field along *x* axis) and *TM* incidence (*E* incident field along *y* axis).

most of the RCS reduction for both *TE* and *TM* polarization falls in correspondence with the frequency band where the infinite *FSS* presents a reflection coefficient reduction higher than 5 dB.

3. DESIGN METHODOLOGY OF THE LOW RCS ANTENNA WITH A THIN BACKING ABSORBER

As previously remarked, in a realistic environment, scatterers located behind the antenna may invalidate the RCS reduction performance achieved by employing a *FSS* ground plane. The goal is therefore to design a thin absorbing structure able to dissipate the energy flux intersected by the *FSS* ground plane of the microstrip array. The main requirements to be fulfilled by the presence of the absorber are the following:

- Reduced impact on the overall thickness of the structure;
- Preservation or, if possible, improvement of the above described RCS reduction performance;
- Preservation or, if possible, improvement of the radiation performance of the antenna with solid ground.

Since the absorbing panel cannot have a direct contact with the metallic *FSS*, a foam spacer is needed to separate it from the frequency selective surface. The evaluation of the optimal thickness of the foam spacer is therefore investigated in detail in the following. The absorbing layer is designed according to the theory of the thin High-Impedance
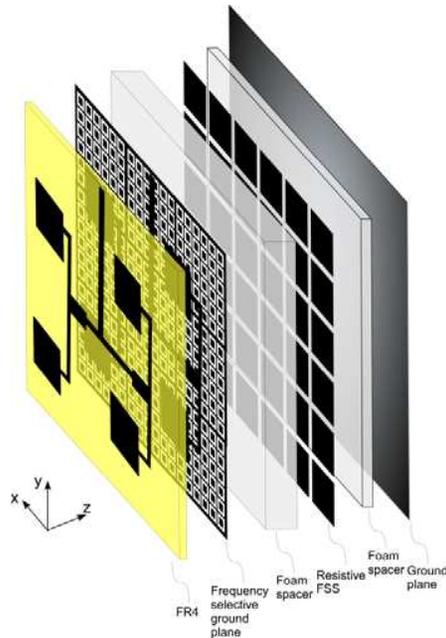
Figure 3. 3D sketch of the proposed structure.

Surfaces (HISs) absorbers [20] in order to keep the encumbrance of the panel as low as possible. A 3D sketch of the proposed structure is shown in Fig. 3.

To perform the study, the transmission line model of the multilayer is adopted since it provides a useful insight. Moreover, it allows a very fast analysis if compared to a full wave simulation which requires several hours for each spacer thickness. The model, reported in Fig. 4, comprises a RLC circuit which represents the resistive *FSS* and a parallel lossless LC circuit referring to the slot ring metallic *FSS*. A similar approach for the analysis of multiple *FSSs* screen has been frequently adopted in the literature [21–24]. It is worthwhile observing that it is not correct to design the absorber as a standalone structure and then to place it at some distance from the hybrid *FSS*. In fact, as it is apparent in Fig. 4, the presence of the metallic *FSS* significantly changes the input impedance of the overall structure that deviates from that of the isolated absorber.

As illustrated in the circuit, the input impedance Z_{spacer} to the right of the foam spacer is in parallel with the impedance of the metallic *FSS*, $ZFSS_{slotring}$. The value of the impedance of the inductive metallic *FSS* as subscript is close to zero at low frequencies and it goes

to infinite at the resonance. At low frequencies the parallel connection is dominated by the low value of $ZFSS_{slotring}$ and the short circuit, necessary for the correct operation of the printed antenna, is ensured. In correspondence of the resonance, the impedance of the inductive *FSS* goes to infinite and the input impedance of the whole system around the resonance can be controlled by the loading impedance of the absorber, Z_{abs} as well as by changing the thickness of the spacer, d_{spacer}.

    The possibility of obtaining an ideal design where the reflection coefficient of the multilayer would be equal to one in correspondence of the antenna bandwidth (up to 4 GHz) and equal to zero in the rest of the band has been initially investigated. Such initial hypothesis allows us to obtain, by means of the equivalent circuit, the optimal impedances in correspondence of two interfaces of the multilayer schematized in Fig. 5. Fig. 5(b) shows the optimal value of the Z_{abs} impedance that should be exhibited by the absorbing layer for different values of the foam spacer thickness. The discontinuity observed at 4 GHz is due to the ideal hypothesis here applied. The real part of the reported input impedance is attainable by a thin narrow-band absorber, but the imaginary part is not a physically realizable impedance since it does not satisfy the Hilbert transform, that is, it does not spin counter clockwise on the Smith chart [25]. A thin electromagnetic absorber with a patch type unit cell is chosen to match the optimal impedance since it allows obtaining the larger operating bandwidth for a given thickness of the substrate [26]. The periodicity of the resistive *FSS* is chosen to be commensurate with the periodicity of the metallic *FSS* (the ratio of the periods is a rational number) both for practical issues and for allowing the full-wave analysis of the multilayer structure by means of periodic boundary conditions. The
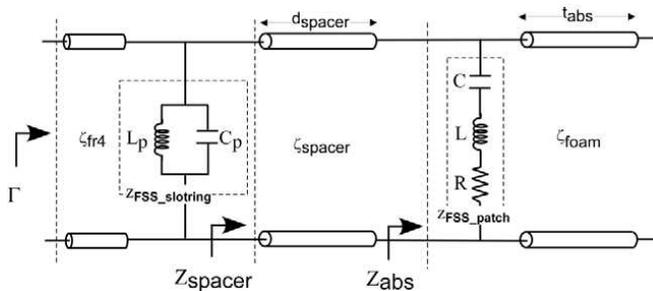

Figure 4. Transmission line model of the multilayer structure. Optimal values of d_{spacer} and t_{abs} obtained for the final design are 3 mm and 4 mm, respectively. $\zeta_{foam} = \zeta_{spacer} = 377/\sqrt{1.05 - j0.017}$.

inductances, the capacitances and the resistor of the FSSs used in the equivalent circuit are derived by following the procedure shown in [20, 27] respectively. The values are summarized in Table 1 and in Table 2. The patch *FSS* is approximated with a LC series circuit instead of a single capacitor as in [28] since the analysis extends beyond the HIS resonance [29].

An example of the input impedance that can be obtained by a thin absorbing panel working within the investigated frequency range is reported in Fig. 6. As is evident, the imaginary part is inductive
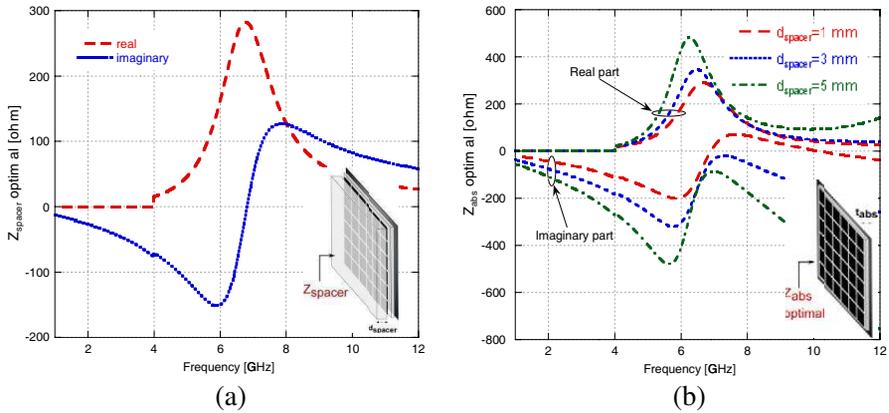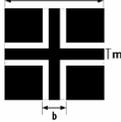

Figure 5. Optimal input impedances at two different interfaces of the multilayer for achieving perfect reflection up to 4 GHz and complete absorption after 4 GHz at the input of the system: (a) Real and imaginary parts of the optimal input impedance before the foam spacer. (b) Real and imaginary parts of the optimal impedance at the input of the loading absorber for different values of the foam spacer.

Table 1. Lumped circuit parameters which characterize the resistive *FSS* composing the absorbing layer.

Resistive patch *FSS*		
Actual parameters		
D [mm]	w [mm]	Surface Res. [Ω/sq]
16	2	50
Lumped parameters		
L [nH]	C [pF]	R [Ω]
0.44	0.16	65

Table 2. Lumped circuit parameters which characterize the metallic
slot ring *FSS* composing the ground plane.

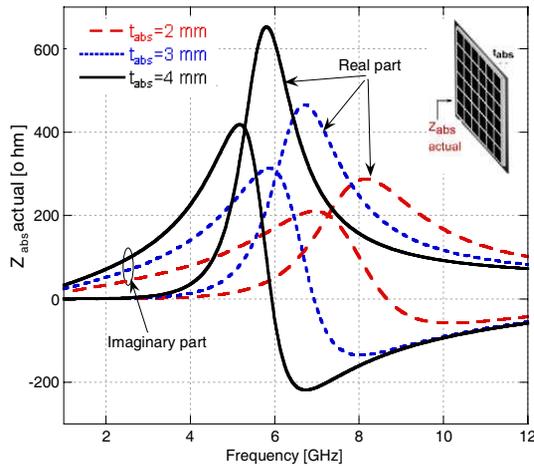| Slot ring *FSS*			
	Actual parameters		
	T [mm]	m [mm]	b [mm]
	8	1	2
	Lumped parameters		
	L_p [nH]	C_p [pF]	
	1.94	0.217	

Figure 6. Input impedance of a physical realizable thin absorbing
panel (Z_{abs}-actual) based on a resistive high-impedance surface.

at low frequencies and becomes capacitive after the resonance. By
comparing the feasible input impedances with the optimal one, as
illustrated in Fig. 7, it can be noticed that the real part of the optimal
impedance can be reproduced quite well after 6 GHz with the 4 mm
thick absorber and, in this range, the imaginary part of the feasible
impedance intersects two times the curve of the optimal impedance.
This means that the chosen physically-realizable backing absorber
allows obtaining two frequency points where the incoming energy is
absorbed by the multilayer instead of one as in the case of the free
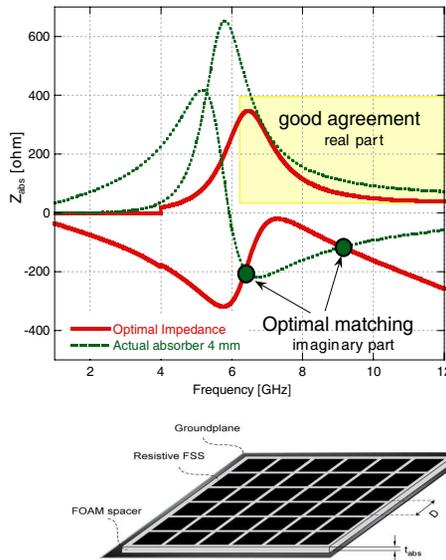space backing.

Figure 7. Comparison between the real and imaginary parts of the input impedance required for an optimal matching and the actual input impedance of a 4 mm thick HIS absorber with $D = 16$ mm. The optimal matching is achieved in the two points where the imaginary part of the optimal impedance and the actual one intersect since the real part of the impedances agree in the shaded zone. Optimal impedance means a configuration leading to perfect reflection of the multilayer up to 4 GHz and complete absorption after 4 GHz.

4. NUMERICAL RESULTS

In this section, the multilayer configuration comprising the metallic *FSS* printed on a 2 mm FR4 substrate backed by the foam spacer and then by the ultra-thin absorbing structure is analyzed as an infinite extent structure. Indeed, as shown in Section 2, the most of the RCS reduction of the finite size array appears in correspondence with the frequency band where the infinite backing *FSS* presents a reflection coefficient lower than 5.0 dB. By applying the same criteria in this case, the reflection coefficient of the *FSS* backed by the absorber is studied for defining the best foam spacer thickness and absorber parameters.

The thin absorber configuration located behind the metallic *FSS* is composed by a resistive patch array *FSS* placed at 4 mm from a ground plane. The unit cell period D of the resistive *FSS* is equal to 16 mm which is twice the period of the metallic *FSS* and the dimension
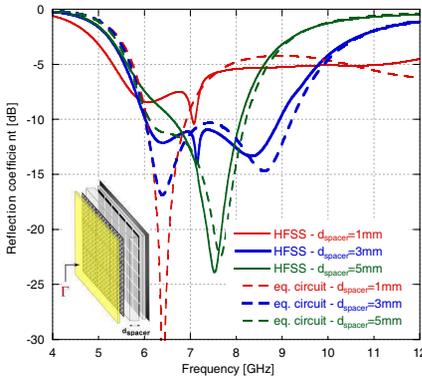
Figure 8. Reflection coefficient at the input of the infinite multi-layer structure. The approximate results obtained by the equivalent circuit are compared against the full-wave results.
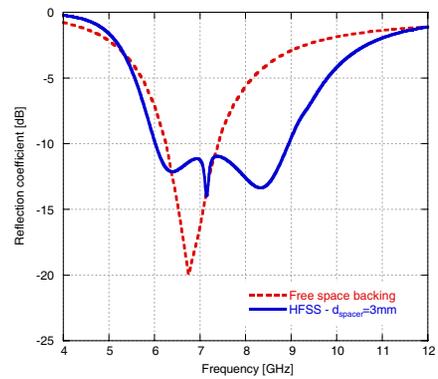
Figure 9. Reflection coefficient of the infinite *FSS* backed either by free space or by the thin absorbing structure. The results are obtained by using Ansoft HFSS.

of the resistive patch is equal to 14/16 of the periodicity D. The reflection coefficient of the multilayer structure computed both with the equivalent circuit analysis and by full-wave simulations is reported in Fig. 8 for three different foam spacings.

The results obtained by the equivalent circuit agree quite well with the full-wave ones considering that, when the thickness of the spacer is quite low, some deviations are introduced by the interaction of the high order Floquet modes between the closely coupled FSSs that the equivalent circuit does not take into account [30, 31]. The influence of the high-order modes is particularly evident for spacer thickness lower than $\lambda/15$, that is, $d_{spacer} = 1$ mm. A slight residual discordance between the approximated models and full-wave solution is always present in model based approaches as the present one, also in absence of higher order Floquet modes interaction. However, the estimates provided by the equivalent circuit are very useful at least for a qualitative estimate of the performance since they accurately reproduce the presence of the two absorbing peaks discussed in the previous section.

The absorption bandwidth for a foam spacer thickness of 3 mm is the widest one and, as is evident from Fig. 9, it is even larger than the one obtained with the free space loading. Once the best configuration of the multilayer structure is selected, the analysis provided by the equivalent circuit is then refined by a full-wave approach.
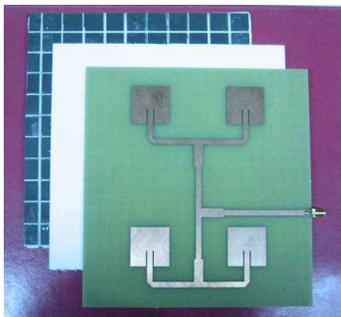
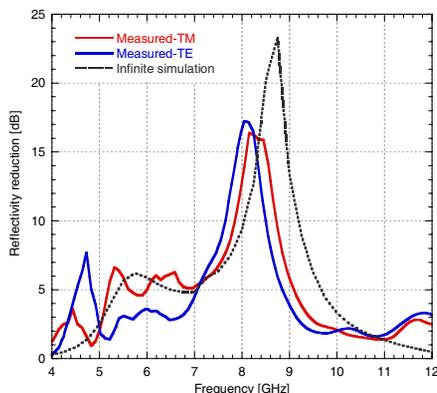**Figure 10.** A picture of the manufactured prototype of the low RCS antenna.

Figure 11. Comparison between the simulated reflection coefficient of the infinite *FSS* and the measured reduction of the array reflectivity for *TE* and *TM* incidence.

5. MEASURED RESULTS ON THE FINITE PROTOTYPE

A small 2×2 microstrip patch array antenna baked by the foam spacer and by the resistive high-impedance surface absorber has been manufactured for testing the RCS and the radiating performance of the antenna [32]. A picture of the manufactured prototype is reported in Fig. 10. The thickness of the spacer separating the resistive *FSS* from the metallic *FSS* is 3 mm while the thickness of the absorber spacer is 4 mm. The side length of the resistive patches is equal to 14.5 mm while the periodicity is 16 mm. The geometrical parameters of the metallic slot ring *FSS* are the same as reported in Table 2. In the final design the three parts are overlapped and glued together.

5.1. RCS Performance

The resistive *FSS* has been realized by silk printing a resistive ink on a thin (0.2 mm) FR4 dielectric substrate. The resistive ink, Minico M2000, is produced by Henkel corporation. Once manufactured, the surface resistivity of the patches has been measured by a transmission/reflection technique in a waveguide [33] and it resulted $35 \, \Omega/\text{sq}$ instead of $50 \, \Omega/\text{sq}$ as expected. The technology to realize these types of absorber are currently under research and validation, especially for what concerns the employed paints, but this clearly

outgoes the scope of the present paper. However, even if the fabricated sample is not the optimal one, it is anyway suitable for testing our design procedure. The efficiency of the proposed design approach is proved by comparing the reflection coefficient of the finite antenna sample backed by the resistive absorber with the reflection obtained by the array backed by a perfect electric ground plane. In Fig. 11, the measured reflectivity reduction of the prototype is compared to the one of the infinite multilayer structure placed behind the radiating array of metallic patches. The results are in good agreement considering that the reflection coefficient of the infinite structure is obtained without taking into account the presence of the patch array. The effects of the edge diffraction, due to the finite ground plane, are obviously not considered in the infinite multilayer structure and this causes the different behavior at the low frequencies since the structure size becomes only three wavelengths. Given the difficulty in the realization of an accurate surface resistance value, the final design could be refined through an optimization procedure oriented to find the best suitable foam spacers and the optimal metallic *FSS* starting from the practically attainable surface resistance of the patch array.

5.2. Radiation Performance

A potential drawback in replacing the ground plane with the finite *FSS* might result in the modification of the array patterns and its return loss. The S_{11} of the antenna with the modified ground plane is compared against the one of the reference antenna with metal ground in Fig. 12. The proposed solution is quite robust since the frequency
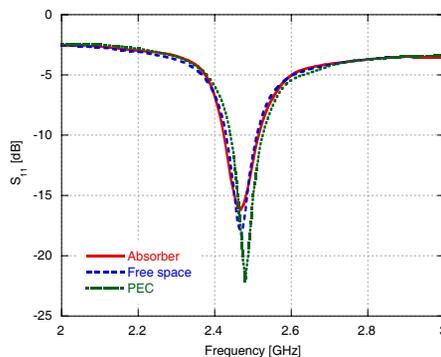

Figure 12. Measured S_{11} of the array with continuous ground plane, with hybrid *FSS* ground plane backed both by free space and by the absorber.
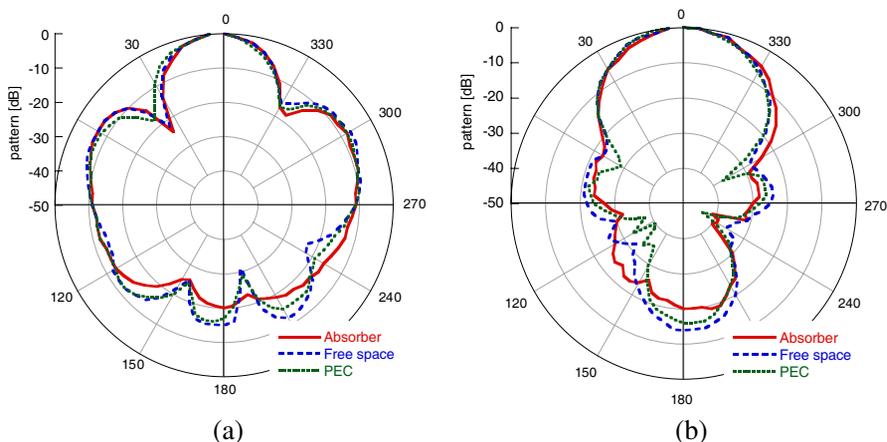
Figure 13. Comparison between the measured radiation patterns of the array on the *E*-plane (a) and *H*-plane (b) at 2.45 GHz.

response of the modified structure agrees quite well with the original one. The resonance frequency of the antenna is 2.45 GHz.

The radiation patterns of the antenna array with the conventional solid ground, the hybrid *FSS* ground backed by free space and the hybrid *FSS* ground backed by the absorber are illustrated in Fig. 13 at the resonance frequency. The gain of the three antenna configurations at broadside is very similar since the power received by the reference horn antenna in the measurement setup is the same. It is instead apparent that the configuration backed by the absorber presents a considerably lower back radiation even with respect to the case with solid PEC ground. The favorable behavior is due to the presence of the backing absorber that reduces the effect of the surface waves travelling on the structure [34].

6. CONCLUSIONS

The use of a suitable hybrid PEC-FSS ground plane backed by a thin absorbing structure has been proved to be an effective means of radar cross section reduction preserving, at the same time, the radiation performance of the antenna. The presence of the absorbing layer below the patterned *FSS* ground allows absorbing the incoming out of band energy that, once flowed through the *FSS*, can be scattered by objects located in the proximity of the antenna.

The novel solution allows to enlarge the bandwidth in which the signature reduction is operated with respect to the free space design.

Moreover, a decrease of the antenna back radiation, even with respect to the metallic ground plane case, is obtained. A prototype of the multilayer structure has been manufactured and the measured results confirm all the speculations and assess the estimated performance.

REFERENCES

1. Knott, E. F., J. F. Shaeffer, and M. T. Tuley, *Radar Cross Section*, 2nd edition, SciTech Publication, Raleigh, NC, 2004.

2. Kraus, J. D. and R. J. Marhefka, *Antennas*, 3rd edtion, Mc Graw-Hill, New York, 2002.

3. Volakis, J. L., A. Alexanian, and J. M. Lin, "Broadband RCS reduction of rectangular patch by using distributed loading," *Electron. Lett.*, Vol. 28, No. 25, 2322–2323, 1992.

4. Li, Y., H. Zhang, Y. Fu, and N. Yuan, "RCS reduction of ridged waveguide slot antenna array using EBG radar absorbing material," *IEEE Antennas Wireless Propag. Lett.*, Vol. 7, 473–476, 2008.

5. Wang, F. W., S. X. Gong, S. Zhang, X. Mu, and T. Hong, "RCS reduction of array antennas with radar absorbing structures," *Journal of Electromagnetic Waves and Applications*, Vol. 25, No. 17–18, 2487–2496, 2011.

6. Xu, H.-Y., H. Zhang, X. Yin, and K. Lu, "Ultra-wideband Koch fractal antenna with low backscattering cross section," *Journal of Electromagnetic Waves and Applications*, Vol. 24, No. 17–18, 2615–2623, 2010.

7. Jiang, W., T. Hong, Y. Liu, S.-X. Gong, Y. Guan, and S. Cui, "A novel technique for radar cross section reduction of printed antennas," *Journal of Electromagnetic Waves and Applications*, Vol. 24, No. 1, 51–60, 2010.

8. Gustafsson, M., "RCS reduction of integrated antenna arrays and radomes with resistive sheets," *IEEE Antennas and Propag. Symp.*, 3479–3482, July 2006.

9. Jiang, W., Y. Liu, S. Gong, and T. Hong, "Application of bionics in antenna radar cross section reduction," *IEEE Antennas Wireless Propag. Lett.*, Vol. 8, 1275–1278, 2009.

10. Pozar, D. M., "RCS reduction for a microstrip antenna using a normally biased ferrite substrate," *IEEE Microwave Guided Wave Lett.*, Vol. 2, 196–198, 1992.

11. Jang, H.-K., W.-J. Lee, and C.-G. Kim, "Design and fabrication of a microstrip patch antenna with a low radar cross section in the X-band," *Smart Materials and Structures*, Vol. 20, 015007, 2011.

12. Hansen, R. C., "Relationships between antennas as scatterers and as radiators," *Proc. IEEE*, Vol. 77, No. 5, 659–662, May 1989.

13. Bletsas, A., A. G. Dimitriou, and J. N. Sahalos, "Improving backscatter radio tag efficiency," *IEEE Trans. on Microwave Theory and Techniques*, Vol. 58, No. 6, 1502–1509, Jun. 2010.

14. Xu, H.-Y., H. Zhang, K. Lu, and X.-F. Zeng, "A holly-leaf-shaped monopole antenna with low RCS for UWB application," *Progress In Electromagnetics Research,* Vol. 117, 35–50, 2011.

15. Misran, N., R. Cahill, and V. F. Fusco, "RCS reduction technique for reflectarray antennas," *Electron. Lett.*, Vol. 39, 1630–1631, Nov. 2003.

16. Li, H., B.-Z. Wang, G. Zheng, W. Shao, and L. Guo, "A reflectarray antenna backed on *FSS* for low RCS and high radiation performances," *Progress In Electromagnetics Research C*, Vol. 15, 145–155, 2010.

17. Ren, L.-S., Y.-C. Jiao, J.-J. Zhao, and F. Li, "RCS reduction for a FSS-backed reflectarray using a ring element," *Progress In Electromagnetics Research Letters*, Vol. 26, 115–123, 2011.

18. Genovesi, S. and A. Monorchio, "Low profile array with reduced radar cross section," *2010 URSI International Symposium on Electromagnetic Theory (EMTS)*, 799–802, Aug. 16–19, 2010.

19. Genovesi, S., F. Costa, and A. Monorchio, "Low profile array with reduced radar cross section by using frequency selective surfaces," *IEEE Trans. on Antennas and Propagation*, Vol. 60, No. 5, 2012.

20. Costa, F., A. Monorchio, and G. Manara, "Analysis and design of ultra thin electromagnetic absorbers comprising resistively loaded high impedance surfaces," *IEEE Trans. on Antennas and Propagation*, Vol. 58, No. 5, 1551–1558, 2010.

21. Erdemli, Y. E., K. Sertel, R. A. Gilbert, D. E. Wright, and J. L. Volakis, "Frequency-selective surfaces to enhance performance of broad-band reconfigurable arrays," *IEEE Trans. on Antennas and Propagation*, Vol. 50, No. 12, 1716–1724, Dec. 2002.

22. Sarabandi, K. and N. Behdad, "A frequency selective surface with miniaturized elements," *IEEE Trans. on Antennas and Propagation*, Vol. 55, 1239–1245, 2007.

23. Al-Joumayly, M. and N. Behdad, "A new technique for design of low-profile, second-order, bandpass frequency selective surfaces,"

IEEE Trans. on Antennas and Propagation, Vol. 57, 452–459, 2009.

24. Costa, F. and A. Monorchio, "Design of subwavelength tunable and steerable fabry-perot/leaky wave antennas," *Progress In Electromagnetics Research*, Vol. 111, 467–481, 2011.

25. Newman, E. H., "Real frequency wideband impedance matching with non-minimum reactance equalizers," *IEEE Trans. on Antennas and Propagation*, Vol. 53, No. 11, 3597–3603, Nov. 1991.

26. Costa, F., S. Genovesi, and A. Monorchio, "On the bandwidth of high-impedance frequency selective surfaces," *IEEE Antennas Wireless Propag. Lett.*, Vol. 8, 1341–1344, 2009.

27. Costa, F., A. Monorchio, and G. Manara, "Efficient analysis of frequency selective surfaces by a simple equivalent circuit model," *IEEE Antennas and Propagation Magazine*, Vol. 54, 2012.

28. Luukkonen, O., C. Simovski, G. Granet, G. Goussetis, D. Lioubtchenko, A. V. Räisänen, and S. A. Tretyakov, "Simple and accurate analytical model of planar grids and high-impedance surfaces comprising metal strips or patches," *IEEE Trans. on Antennas and Propagation*, Vol. 56, No. 6, 1624–1632, 2008.

29. Kim, S.-H., T. T. Nguyen, and J.-H. Jang, "Reflection characteristics of 1-D EBG ground plane and its application to a planar dipole antenna," *Progress In Electromagnetics Research*, Vol. 120, 51–66, 2011.

30. Munk, B. A., *Frequency Selective Surfaces — Theory and Design*, John Wiley & Sons, New York, 2000.

31. Tretyakov, S., *Analytical Modelling in Applied Electromagnetics*, Artech House, Boston, 2003.

32. Zhang, Y., B. Z. Wang, W. Shao, W. Yu, and R. Mittra, "Artificial ground planes for performance enhancement of microstrip antennas," *Journal of Electromagnetic Waves and Applications*, Vol. 25, No. 4, 597–606, 2011.

33. Glover, B., K. Kirschenmann, and K. W. Whites, "Engineering R-card surface resistivity with printed metallic patterns," *Proceedings Metamaterials' 2007 International Congress on Advanced Electr. Materials in Microwaves and Optics*, 621–624, Rome, Italy, Oct. 22–26, 2007.

34. Bianconi, G., F. Costa, S. Genovesi, and A. Monorchio, "Optimal design of dipole antennas backed by a finite high-impedance screen," *Progress In Electromagnetics Research C*, Vol. 18, 137–151, 2011.